

Short communication

A bi-functional micro-porous layer with composite carbon black for PEM fuel cells

Xiaoli Wang^{a,b}, Huamin Zhang^{a,*}, Jianlu Zhang^c, Haifeng Xu^{a,b},
Xiaobing Zhu^{a,b}, Jian Chen^a, Baolian Yi^a

^a Key Material Laboratory for PEMFCs, Dalian Institute of Chemical Physics, CAS, Dalian 116023, China

^b Graduate School of the Chinese Academy of Sciences, CAS, Beijing 100039, China

^c Institute for Fuel Cell Innovation, National Research Council Canada, Vancouver, BC, Canada V6T 1W5

Received 9 May 2006; received in revised form 22 June 2006; accepted 22 June 2006

Available online 5 September 2006

Abstract

Micro-porous layers (MPLs) prepared with different carbon materials were investigated. By the analysis of morphology, wettability and pore structure, the characteristics of each gas diffusion layer (GDL) were compared. A high efficiency bi-functional MPL with composite carbon black consisting of 20 wt.% Black Pearls 2000 carbon and 80 wt.% Acetylene Black carbon is proposed to enhance the transportation of both reactant gases and liquid water. Furthermore, a novel GDL with a gradient in porosity formed by adding MPLs with different carbon loadings on the catalyst layer side and on the flow field side is suggested for improved liquid water removal.

© 2006 Elsevier B.V. All rights reserved.

Keywords: Proton exchange membrane fuel cell; Gas diffusion layer; Bi-functional micro-porous layer; Composite carbon black; Gradient porosity

1. Introduction

Proton exchange membrane fuel cells (PEMFCs) are promising alternative power sources for stationary and mobile applications. The porous gas diffusion layer (GDL) consisting of a gas diffusion backing (GDB) and a micro-porous layer (MPL) plays an important role in the PEMFC by affecting the diffusion of reactants and water, and the conduction of electrons. An MPL composed of carbon black powder and hydrophobic agent such as PTFE is applied on one side or two sides of the GDB, which is intended to provide a proper pore structure and wettability to allow effective gas and water transport and furthermore decrease the electric contact resistance between the GDL and the adjacent components.

The MPL has a critical role in achieving high performance for the PEMFC. In modelling analysis, numerous studies concentrated on two-phase flow and transport in GDLs [1–11]. Some favourable parameters involving porosity, thickness, wet-

tability of GDLs and ex-situ operation condition had been drawn from the mathematical calculations [1–4]. It was suggested that the presence of a thin and highly hydrophobic MPL could decrease the catalyst layer liquid saturation significantly. Further understanding of the mechanism of mass transport in the micro-structure of GDLs is important for cell performance enhancement.

Prior research has focused on the components of the MPL such as the carbon black and the hydrophobic agent and optimizing the content and thickness of MPL [12–18]. Various types of carbon black were employed to prepare MPLs with different morphologies and pore structures [19–22]. In previous work, the MPL was usually prepared with a single type of carbon black and the pores formed were of one distribution. And also few papers were concerned with the differences of the required MPLs on the catalyst layer side and on the flow field side [20,23]. The mass transport problem in the GDL is still serious.

In this paper, a novel MPL made with composite carbon powder of Acetylene Black carbon and Black Pearls 2000 carbon was reported. By adopting the two carbon blacks with greatly different features, a bi-functional pore structure has been designed

* Corresponding author. Tel.: +86 411 8437 9072; fax: +86 411 8466 5057.
E-mail address: zhanghm@dicp.ac.cn (H. Zhang).

which maintains the requirement for good transportation of both reactant gases and liquid water. A new gradient GDL by adding different MPLs on each side of GDB is suggested which exhibits a more reasonable pore structure and higher electronic conductivity to obtain better cell performance.

2. Experimental

2.1. Preparation of membrane electrode assemblies (MEAs)

Gas diffusion layers were prepared using wet-proofed carbon papers (TGPH-030, Toray) as GDBs. To form the MPL, an alcohol suspension of carbon powder and 10 wt.% PTFE emulsion were stirred thoroughly by an ultrasonic machine and then was spread onto the GDB with a doctor blade to form the precursor for the MPL, then the precursor was baked at 240 °C for 30 min, and finally it was sintered at 350 °C for 40 min. The PTFE content in the MPL was 30 wt.% and the detail parameters and the naming of different GDLs are presented in Table 1. The anode GDLs used in the experiments in this paper are same, with SGL carbon papers as GDBs and Vulcan XC-72 as MPL carbon blacks.

The catalyst-coated membrane (CCM) was prepared as follows: dispersing Pt/C catalyst (46.1 wt.%, TKK, Tanaka Kikinzoku Kogyo K.K.), Nafion solution (5 wt.%, DuPont) in isopropanol to form a homogeneous mixture, spraying the mixture directly onto each side of a Nafion 1035 membrane and then drying the as-prepared CCM at room temperature for 24 h to evaporate the residual solvents. The Nafion loading in the catalyst layer was 25 wt.% and Pt loading was 0.25 mg cm⁻² for both cathode and anode. To stabilize the catalyst layer and enhance the contact between catalyst layer and membrane, the CCM was firstly hot-treated at 160 °C under a pressure of 1.0 MPa for 5 min and then sandwiched between two gas diffusion layers followed by a hot-pressing procedure at 160 °C and 10 MPa for 1 min to form a membrane electrode assembly (MEA).

2.2. Evaluation of single cells

MEAs (with 5 cm² active area) were evaluated in single cells at 80 °C under 0.2 MPa. The reactant gases, hydrogen and air, were externally humidified before entering the single cells by bubbling them through the water at 90 and 85 °C, respectively. Constant reactant flow rate of 50 ml min⁻¹ for hydrogen and 200 ml min⁻¹ for air was used. The cell voltages versus current densities curves were obtained with a homemade electrical load.

Table 1
Parameters of different gas diffusion layers

GDLs	Types of carbon powders	X Y ^a (mg cm ⁻²)	Total carbon loadings (mg cm ⁻²)
AB	Acetylene Black carbon	0.5 0.5	1.0
BP	Black Pearls 2000 carbon	0.5 0.5	1.0
CC1	80 wt.% Acetylene Black + 20 wt.% Black Pearls 2000	0.5 0.5	1.0
CC2	80 wt.% Acetylene Black + 20 wt.% Black Pearls 2000	0.7 0.3	1.0
CC3	80 wt.% Acetylene Black + 20 wt.% Black Pearls 2000	1.0 0.0	1.0

^a (X|Y) is indicated a GDL, where X is the carbon loading in MPL for catalyst layer side, and Y is the carbon loading in MPL for flow field side.

2.3. Physical characteristics

BET surface areas, pore volumes of the different carbon powders were determined by an ASAP-2010 (Micromeritics) physisorption system using N₂ as the adsorbate at 77 K. The morphological characteristics of the micro-porous surface layer were examined using scanning electron microscopy (SEM, JSM-6360LV, JEOL Co.). The information on the internal structure of gas diffusion layers was determined by mercury-intrusion porosimeter (Autopore 9510, Micromeritics Inc.)

3. Results and discussion

3.1. Physical properties of carbon powders

The physical properties of the carbon powders chosen for this investigation are summarized in Table 2. The surface area varied over a large range from 62.0 m² g⁻¹ for Acetylene Black to 1501.8 m² g⁻¹ for Black Pearls 2000. This can be explained by the tremendous difference in pore volume and pore size distribution as shown in Fig. 1. The Black Pearls 2000 was abundant with all-size pores and revealed the largest cumulative pore volume. Acetylene Black had the lowest pore volume and no special peak in any pore range. As for the composite carbon powder (80 wt.% Acetylene Black and 20 wt.% Black Pearls 2000), it showed the combined characteristics of the two original materials with a surface area of 335.3 m² g⁻¹. The adding of certain Black Pearls 2000 to Acetylene Black increased the pore volume with diameters less than 5 nm compared to Acetylene

Table 2
Physical parameters of different carbon powders

Types of carbon powder	Source	Surface area (m ² g ⁻¹)	Particle size (nm)	Meso- and macro-pore volume ^a (cm ³ g ⁻¹)	Micro-pore volume ^b (cm ³ g ⁻¹)
Acetylene Black	Acetylene	62.0	42.0	0.23	0.0045
Black Pearls 2000	Oil-furnace	1501.8	15.0	2.37	0.2191
Composite carbon	–	335.3	–	0.67	0.0412

^a BJH desorption cumulative volume of pores between 1.7000 and 300.0000 nm diameter.

^b *t*-Plot micropore volume.

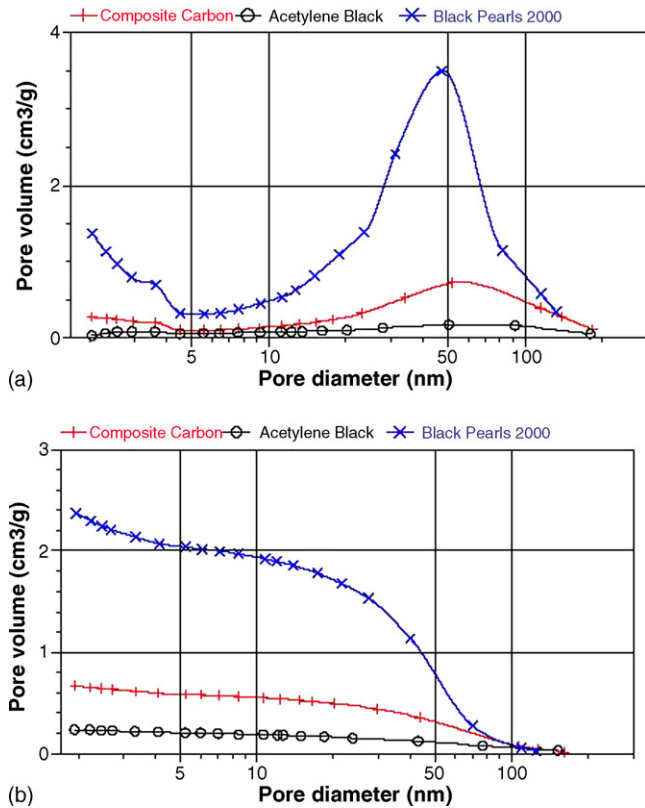


Fig. 1. Pore size distribution of carbons: (a) BJH desorption $dV/d\log(D)$ pore volume; (b) BJH desorption cumulative pore volume.

Black and showed a similar peak at 50 nm to that of Black Pearls 2000.

3.2. Characteristics of GDLs with different MPLs

SEM images of MPLs with different carbon powders are shown in Fig. 2. It can be seen that MPL made with Acetylene Black showed a homogeneous and porous surface with small agglomerates of carbon powder and PTFE. The MPL using Black Pearls 2000 presented the highest compactness of the carbon structure and a few larger cracks due to its smaller pore size. Fig. 2(c) shows the surface morphology of MPL with composite carbon. Indeed, moderate characteristics were observed. The layer appeared to be more uniform and had finer pores.

The pore size distribution curves of the GDL samples were measured with mercury-intrusion porosimeter and are compared in Fig. 3. To identify the structural features in different pore size ranges, the pores in the GDLs are divided according to size into three classes, namely: macro-pores with pore diameter of 7–70 μm , meso-pores in the range of 0.05–7 μm , and micro-pores below 0.05 μm . Note that the definition of the pore range is based on the porosimetry data for the GDL investigated and is different with the general criteria. To discriminate the difference of various GDLs clearly, the comparison of the three size pores for each GDL is presented in Fig. 4.

Reactant transportation from the flow field to the catalyst layer is mainly by diffusion and partly by convection. Diffusional gas transport in the porous media occurs primarily through

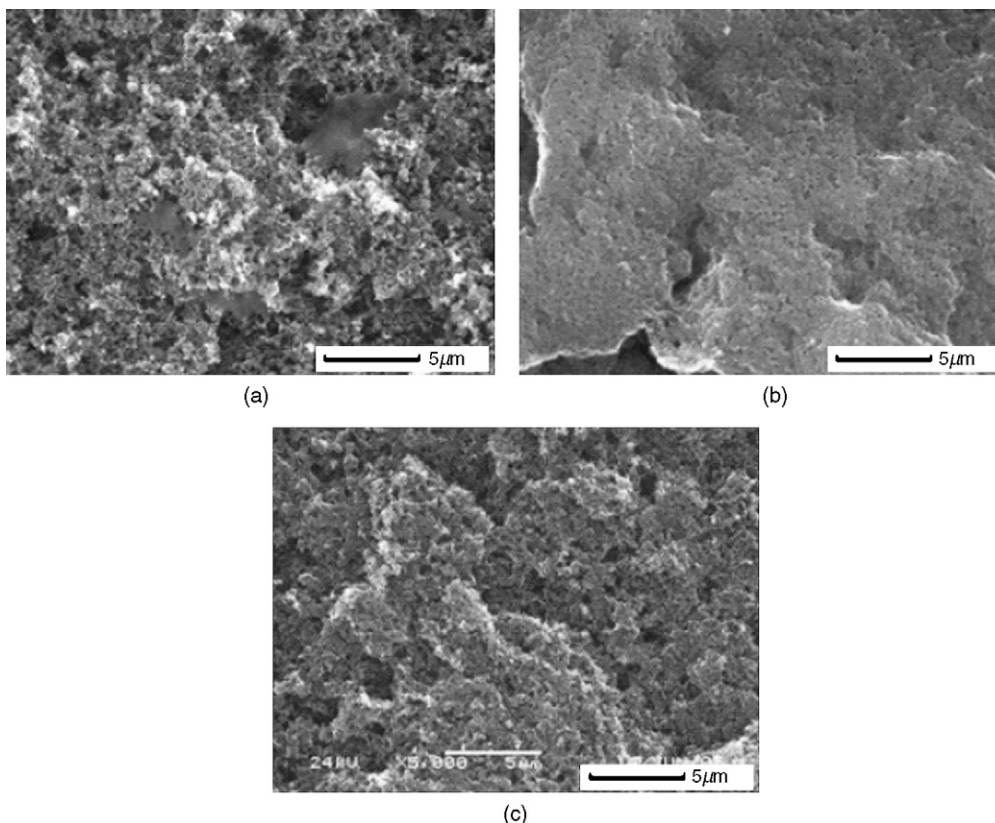


Fig. 2. Scanning electron micrographs of different MPLs: (a) AB; (b) BP; and (c) CC1.

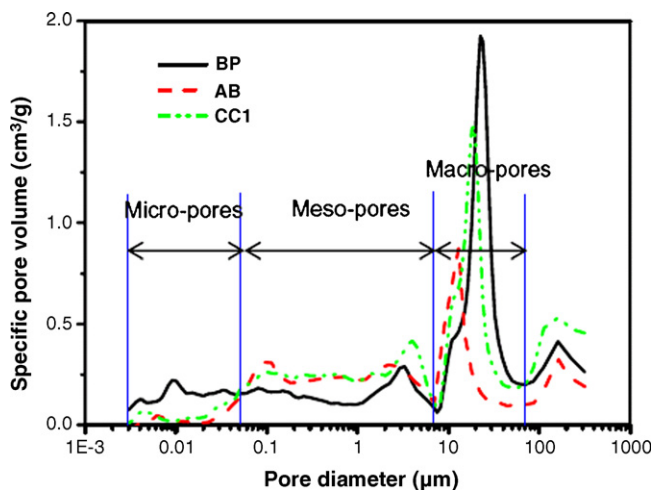


Fig. 3. Specific pore-size distribution of each GDL obtained from mercury intrusion porosimetry measurements.

two processes: Bulk diffusion and Knudsen diffusion. At standard temperature and pressure, the mean free path of nitrogen is 67.6 nm, while that of oxygen is 73.6 nm, therefore the mean free path of air is approximately 70 nm. Bulk diffusion in the pores dominates when the pore diameter is bigger than one hundred times the mean free path or 7 μm , while Knudsen diffusion dominates when the pore diameter is smaller than a tenth of the mean free path or 0.007 μm . Any pore diameter between these two limits will have the effect of both the Knudsen diffusion and the Bulk diffusion combined [24]. The effective diffusion coefficient in the Bulk regime is as high as three orders of magnitude higher than that in the Knudsen regime. The larger pores are beneficial because they aid Bulk diffusion and convection, which enhance mass transport through the substrate.

Capillary-driven liquid flow through diffusion media may predominate in fuel cell operation, especially in the over-saturated system. According to the Young–Laplace equation, a radius can be related to the capillary pressure and wettability

of a pore by

$$P_c = \frac{2\gamma \cos \theta}{r}$$

where γ is the surface energy of water; θ the contact angle of water with the surface of the pore; P_c the capillary pressure and r the radius of pores. For a hydrophilic pore, the contact angle is $0^\circ \leq \theta < 90^\circ$, and for a hydrophobic pore, the contact angle is $90^\circ < \theta \leq 180^\circ$. The value of r is the largest (smallest) liquid-filled pore radius for a hydrophilic (hydrophobic) pore [25]. Therefore, the larger of the hydrophobic pore, the more easily liquid water is forced into it by the pressure from membrane swelling [26]. The smaller of hydrophilic pore, the more easily liquid is drawn into it driven by the capillary force. While for the hydrophobic meso-pores, liquid water does not easily penetrate because more work is needed to overcome the surface energy. So the hydrophobic meso-pores are kept free for gas transport.

According to the above analysis, the pore size distribution and the wettability of the pore-walls are the two most influential factors in the gas/water transportation. Black Pearls 2000 had a high surface area and capability to adsorb water internally [27] and thus the MPL using Black Pearls 2000 was more hydrophilic. Moreover, the most micro- and macro-pores and the least meso-pores of BP (as can be seen from Fig. 4) aggravated the occupation of liquid water in GDL and weakened the diffusion of gases, from which we could infer that BP was prone to be “flooded”. While the surface of Acetylene Black was comparatively hydrophobic [28] and the MPL using Acetylene Black could provide sufficient hydrophobic pores for gas passage. Furthermore, AB possessed comparative more meso-pores compared to that of BP, which could offer a great lot of passageways for gas diffusion. The disadvantage of AB was that less hydrophilic micro-pores were presented as shown in Fig. 4, which might hinder liquid water removal from the cell. In the case of CC with the composite carbon black, it increased appropriately the micro-pores for water flow by the adding of a small number of Black Pearls 2000 in Acetylene Black while kept similar hydrophobicity to that of AB [28]. The relatively more meso- and macro-pores ensured the good transportation of reactants.

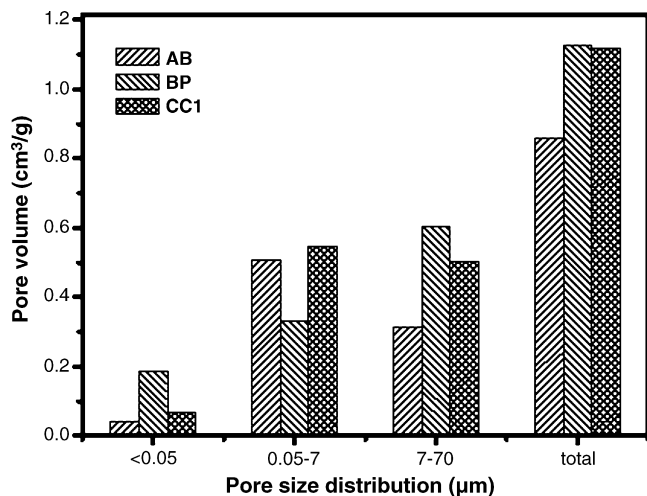


Fig. 4. Comparison of pores in different range of each GDL.

3.3. Cell performance of electrode with various GDLs

The polarization curves of single cells with different GDLs are shown in Fig. 5. A constant flow rate was used to help emphasize the mass transport effects and to make the limiting current easier to reach in the polarization curves. In fact, 200 ml min^{-1} for air was sufficient and no obvious mass transport losses appeared in the activation polarization and ohmic polarization control regions. As shown in Fig. 5, the electrode with AB showed a higher limiting current than BP, which exhibited severe mass transport polarization even at a low current density of 650 mA cm^{-2} . Electrodes with CC1, containing composite carbon of 80 wt.% Acetylene Black and 20 wt.% Black Pearls 2000 in MPL, presented the best performance with the break point of voltage at 1000 mA cm^{-2} . The different limiting

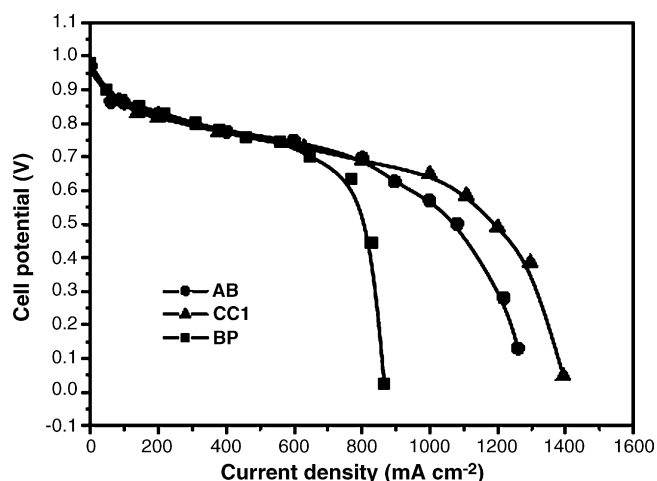


Fig. 5. Single cell performance of electrodes with different GDLs whose MPLs contained Acetylene Black, composite carbon black (80 wt.% Acetylene Black + 20 wt.% Black Pearls 2000) and Black Pearls 2000, respectively. $X|Y=0.5|0.5 \text{ mg cm}^{-2}$; constant flow rate of 200 ml min^{-1} for air and of 50 ml min^{-1} for hydrogen; cell temperature 80°C , anode humidifier temperature 90°C , cathode humidifier temperature 85°C ; pressure $0.2/0.2 \text{ MPa}$.

currents were mainly due to the difference of mass transport through each GDL because all the other factors were identical including CCMs, anodes, cell assembling pressures and operating conditions.

An explanation of our experimental results can be derived by the analysis above about the characteristics of each GDL. We believe that AB, with the porous structure and higher hydrophobicity, is beneficial to gas diffusion, and reduces the mass transport polarization. But the smaller fraction of micro-pores hinders liquid water removal by capillary-driven forces, which are potential factors in restricting GDL performance especially at high current densities. BP shows severe gas transport limitations through macro-pores which can be ascribed to the stronger hydrophilicity of the Black Pearls 2000. So even at the relatively lower current density, a concentration overpotential is apparent because of the excessive water contained in the GDL. The best cell performance of CC can be explained by the formation of a bi-functional pore structure, which facilitated the transport of both reactants and liquid water. As expected, by combination of the two advantages of raw carbons, the new MPL presented an optimal pore size distribution and suitable wettability, and therefore, an enhanced cell performance was obtained.

3.4. Comparison of single-side and double-side MPL

As seen from Fig. 6, the electrode with single-side MPL on the catalyst layer side, CC3, presented the worst cell performance compared with that using a double-sided MPL, CC1 and CC2. The total carbon loading was kept at 1.0 mg cm^{-2} , so single layer of MPL was relatively thick and more compact which resulted in the relatively lower gas transport capability. Also the absence of MPL on the gas side increased the contact resistance between the GDL and the flow field. The electrode with CC2, a special gradient GDL structure of $0.7|0.3$, showed the best performance by providing a gradually changing porosity from the catalyst

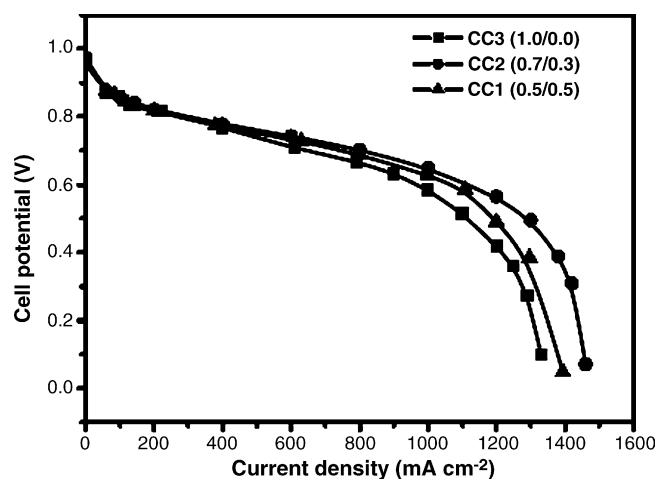


Fig. 6. Cell performance of electrodes with different MPL structure: CC3($X|Y=1.0|0.0$), CC2($X|Y=0.7|0.3$), CC1($X|Y=0.5|0.5$). Constant flow rate of 200 ml min^{-1} for air and of 50 ml min^{-1} for hydrogen; cell temperature 80°C , anode humidifier temperature 90°C , cathode humidifier temperature 85°C ; pressure $0.2/0.2 \text{ MPa}$.

layer side to the flow field side which maintained satisfactory gas/water management.

4. Conclusions

A novel gas diffusion layer with a composite carbon black consisting of 20 wt.% Black Pearls 2000 and 80 wt.% Acetylene Black carbon is reported. The new GDL presents a bi-functional pore structure ensuring good transportation of both reactant gases and liquid water. Indeed, the pore size distribution and wettability are two vital properties of the GDL in affecting the gas/water transportation. We believe that a small number of hydrophilic micro-pores are required in the GDL for the passage of liquid water. Furthermore, largely hydrophobic meso-pores are necessary to ensure sufficient reactants reaching the catalytic sites and a relative more hydrophobic macro-pore distribution is needed for gas transport through bulk diffusion and water flow under a certain pressure. An MPL on double sides of a carbon paper substrate is necessary to maintain satisfactory gas/water management and enhance electron conductivity. The gradient configuration of $0.7|0.3$, with carbon loadings of 0.7 mg cm^{-2} for the catalyst layer side and 0.3 mg cm^{-2} for the flow field side, is preferable.

References

- [1] U. Pasaogullari, C.Y. Wang, *J. Electrochem. Soc.* 151 (2004) A399–A406.
- [2] U. Pasaogullari, C.Y. Wang, *Electrochim. Acta* 49 (2004) 4359–4369.
- [3] J.H. Nam, M. Kaviany, *Int. J. Heat Mass Transfer* 46 (2003) 4595–4611.
- [4] Z. Liu, Z. Mao, C. Wang, *J. Power Sources* 158 (2006) 1229–1239.
- [5] T.E. Springer, T.A. Zawodzinski, S. Gottesfeld, *J. Electrochem. Soc.* 138 (1991) 2334–2342.
- [6] T.E. Springer, M.S. Wilson, S. Gottesfeld, *J. Electrochem. Soc.* 140 (1993) 3513–3526.
- [7] T. Nguyen, R.E. White, *J. Electrochem. Soc.* 140 (1993) 2178–2186.
- [8] W. He, J.S. Yi, T.V. Nguyen, *AIChE J.* 46 (2000) 2053–2064.

- [9] Z.H. Wang, C.Y. Wang, K.S. Chen, *J. Power Sources* 94 (2001) 40–50.
- [10] L. You, H. Liu, *Int. J. Heat Mass Transfer* 45 (2002) 2277–2287.
- [11] D. Natarajan, T.V. Nguyen, *J. Electrochem. Soc.* 148 (2001) A1324–A1335.
- [12] Z. Qi, A. Kaufman, *J. Power Sources* 109 (2002) 38–46.
- [13] L.R. Jordan, A.K. Shukla, T. Behrsing, N.R. Avery, B.C. Muddle, M. Forsyth, *J. Power Sources* 86 (2000) 250–254.
- [14] L.R. Jordan, A.K. Shukla, T. Behrsing, N.R. Avery, B.C. Muddle, M. Forsyth, *J. Appl. Electrochem.* 30 (2000) 641–646.
- [15] J.M. Song, S.Y. Cha, W.M. Lee, *J. Power Sources* 94 (2001) 78–84.
- [16] E. Antolini, R.R. Passos, E.A. Ticianelli, *J. Appl. Electrochem.* 32 (2002) 383–388.
- [17] L. Giorgi, E. Antolini, A. Pozio, E. Passalacqua, *Electrochim. Acta* 43 (1998) 3675–3680.
- [18] J. Moreira, A.L. Ocampo, *Int. J. Hydrogen Energy* 28 (2003) 625–627.
- [19] E. Passalacqua, G. Squadrito, F. Lufrano, A. Patti, L. Giorgi, *J. Appl. Electrochem.* 31 (2001) 449–454.
- [20] E. Antolini, R.R. Passos, E.A. Ticianelli, *J. Power Sources* 109 (2002) 477–482.
- [21] M. Maja, C. Orecchia, M. Strano, P. Tosco, M. Vanni, *Electrochim. Acta* 46 (2000) 423–432.
- [22] M. Neergat, A.K. Shukla, *J. Power Sources* 104 (2002) 289–294.
- [23] G.J.M. Janssen, M.L.J. Overvelde, *J. Power Sources* 101 (1) (2001) 117–125.
- [24] R.H. Perry, D.W. Green, *Perry's Chemical Engineers' Handbook*, 7th ed., McGraw Hill, 1997, pp. 5–55.
- [25] A.Z. Weber, R.M. Darling, J. Newman, *J. Electrochem. Soc.* 151 (2004) A1715–A1727.
- [26] J. Benziger, J. Nehlsen, D. Blackwell, T. Brennan, J. Itescu, *J. Membr. Sci.* 261 (2005) 98–106.
- [27] X. Wang, I.M. Hsing, P.L. Yue, *J. Power Sources* 96 (2001) 282–287.
- [28] X.L. Wang, H.M. Zhang, J.L. Zhang, H.F. Xu, Z.Q. Tian, J. Chen, H.X. Zhong, Y.M. Liang, B.L. Yi, *Electrochim. Acta* 51 (2006) 4909–4915.